Electronic collective modes and instabilities on semiconductor surfaces. II. Theory of electron-phonon interaction

A. Muramatsu
Institute for Theoretical Physics, University of California, Santa Barbara, California 93106

W. Hanke
Max-Planck-Institut für Festkörperforschung, D-7 Stuttgart, West Germany

(Received 8 March 1984)

The phonon self-energy and the dynamical effective charge are expressed in terms of the non–local density-response function $\epsilon^{-1}(\vec{q}+\vec{G}, \vec{q}+\vec{G}', z, z')$ of a surface. The main purpose is to obtain a consistent description of the energy spectra, lifetimes, and amplitudes of electronic surface excitations, such as surface plasmons, excitons, and magnons, which have been discussed in a previous paper with the dynamical (phonon) excitations. An application to the ideal Si(111) surface reveals two types of instabilities of Rayleigh modes, which can be related to relaxation and (2×1) reconstruction.

I. INTRODUCTION

Both the determination of static, structural properties and the study of vibrational excitations on surfaces has recently made significant progress through the application of elaborate experimental techniques, such as low-energy electron diffraction,[1] characteristic energy loss,[2] and scattering of light (He) atoms.[3] From the theoretical point of view, the dynamics of crystal surfaces[4] have so far been exclusively described by empirical models.[5] Here one employs a bulk parametrization of the force constants to extract the surface vibrational modes. These empirical models work well on surfaces of, for example, alkali halides,[5] where the electronic charge distribution surrounding the surface ions as well as their geometrical arrangement is practically unchanged compared to the bulk. This is contrasted by the majority of semiconductor and transition-metal surfaces where the electronic properties are radically different from the bulk. Often this change is accompanied by an instability toward surface reconstruction. Examples are the Si(111) (Ref. 6) and the (001) surfaces of both W and Mo,[7] which display various superstructures as a function of temperature and also adsorbate composition. Here an *a priori* determination of the force constants is needed, which consistently takes both the atomic surface reconstruction and the electronic structure changes into account. The present work aims at such a description.

Our lattice-dynamical formulation focuses on the problem of expressing the phonon self-energy in terms of the response of the surface electrons to an external probe. This approach permits the complete solution of the lattice vibrational problem within the harmonic approximation once the charge of the nuclei (or, in practice, the potential of the ion cores) and a properly defined density-response matrix $\epsilon^{-1}(\vec{q}+\vec{G},\vec{q}+\vec{G}',z,z')$ are known. In a previous paper,[8] hereafter designated as I, a Green's-function formalism for electronic collective modes was developed which facilitates the calculation of ϵ^{-1} in conducting as well as nonconducting solids. The main advantage of this Green's-function formalism lies in the fact that one and the same quantity, i.e., the two-particle propagator, determines a broad range of surface elementary excitations, such as electron-hole excitations, excitons, plasmons, magnons, and phonons. In I this has been exploited to study the spin response of the ideal Si(111) surface. Quantitative calculations for an eight-layer slab displayed an instability of the ideal paramagnetic surface with respect to spin-density waves with wavelength corresponding to (2×1) and (7×7) superstructures. Here we present the density-response theory of surface lattice dynamics, with particular emphasis on semiconductor and transition-metal surfaces where the jellium approximation is not valid, i.e., where density fluctuations are important on a microscopic scale (reflected in the local-field effects). Our paper is organized as follows. In Sec. II, explicit expressions for the phonon self-energy and the surface effective charge are given. The latter has already been derived by one of us for an insulating system, but here we consider a metallic surface such as the ideal Si(111). Section III summarizes results of a phonon calculation for the same eight-layer slab of Si(111), the collective modes and instabilities of which we have already studied in Ref. 8. This calculation gives insight into what drives the ideal Si(111) surface out of its bulk pattern into a structural superstructure. In particular, we find two types of instabilities for the Rayleigh modes: one, which is related to relaxation of the surface layer, and the other being related to the charge-density fluctuations of a (2×1) reconstruction. In the present work the instabilities are found for the ideal surface and we do not predict a new equilibrium for the reconstructed surface lattice structure. However, we emphasized that our dynamical theory can just as well be used to check one of the proposed models for the reconstruction, such as the π-bonded chain model,[9] against experiment.[10] Such a calculation is under way as well as a

many-body study of the optical and photoemission experiments of the (2×1)-Si(111) surface. A final discussion is presented in Sec. IV.

II. THEORETICAL FRAME

We present in this section various aspects of a microscopic theory of surface lattice dynamics. First, we discuss briefly the non—local-dielectric-response function of the surface electronic system, which determines the phonon self-energy in the harmonic approximation. Then an explicit expression of the phonon self-energy itself is presented, and finally we discuss the form of the effective charge for metallic systems, the expression for insulating systems being already given in Refs. 11 and 12.

A. Surface density-response function

The quantity which determines the density-response function is the two-particle Green's function.[13] It was extensively discussed for surface systems in paper I.[8] There we showed that with the help of a local-orbital representation for the one-particle states it is possible to solve the Bethe-Salpeter equation when the irreducible electron-hole interaction is treated in the screened Hartree-Fock approximation.

The susceptibility $\chi(1,2)$ and the two-particle Green's function $G(12,34)$ are related in the following way:[13,14]

$$\chi(1,2)=\sum_{\sigma\sigma'} G_{\sigma\sigma'}(12,2^+1^+) , \tag{2.1}$$

where σ and σ' are spin indices and $\tau_1^+=\tau_1+0^+$. For the polarizability $\tilde{\chi}$ we consider the integral equation for the two-particle Green's function

$$G=G^0+G^0IG , \tag{2.2}$$

where G^0 is the free part, and we include in the irreducible electron-hole interaction (paper I) only those diagrams which do not contain contributions such as the one in Fig. 1(b). This will give all irreducible terms in the two-particle Green's function, the sum of which we call $\tilde{G}$. Then the polarizability is obtained as

$$\tilde{\chi}(1,2)=\sum_{\sigma\sigma'} \tilde{G}_{\sigma\sigma'}(12,2^+1^+) . \tag{2.3}$$

With these definitions, all long-range effects coming from the Coulomb interaction are excluded. They are contained in the susceptibility χ (Ref. 15) which satisfies the following integral equation (Fig. 2):

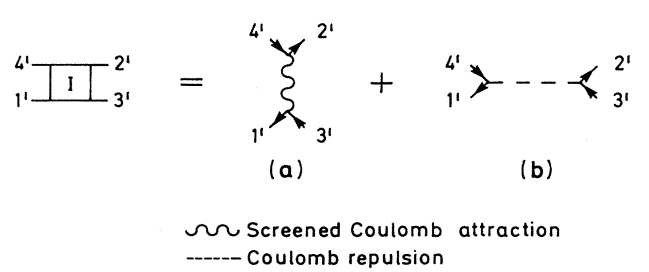

FIG. 1. Irreducible electron-hole interaction I: (a) electron-hole attraction; (b) unscreened exchange.

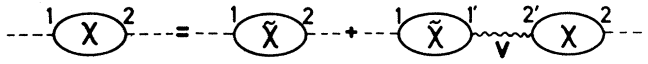

FIG. 2. Integral equation for the susceptibility.

$$\chi(1,2)=\tilde{\chi}(1,2)+\tilde{\chi}(1,1')v(1',2')\chi(2',2) , \tag{2.4}$$

where $v(1',2')$ is the unscreened Coulomb interaction. Because the polarizability $\tilde{\chi}$ can be expressed with the help of Bloch wave functions in the following way:[16]

$$\tilde{\chi}(\vec{r},\vec{r}')=\sum_{n_1\vec{k}_1\cdots n_4\vec{k}_4} \psi_{n_1\vec{k}_1}(\vec{r})\psi^*_{n_2\vec{k}_2}(\vec{r}) \times\tilde{\chi}_{n_1\vec{k}_1,n_2\vec{k}_2,n_3\vec{k}_3,n_4\vec{k}_4} \times\psi_{n_3\vec{k}_3}(\vec{r}')\psi^*_{n_4k_4}(\vec{r}') , \tag{2.5}$$

a local-orbital representation of the wave functions allows us to reach a separable form for $\tilde{\chi}$.[14] In such a representation the Fourier-transformed surface polarizability is given by[8,12,17]

$$\tilde{\chi}(\vec{q}+\vec{G},\vec{q}+\vec{G}';z,z';\omega) =\sum_{ss'} A_s(\vec{q}+\vec{G},z)\tilde{S}_{ss'}(\vec{q},\omega)A^\dagger_{s'}(\vec{q}+\vec{G}';z') , \tag{2.6}$$

where $A_s(\vec{q}+\vec{G},z)$ is a generalized charge-density wave

$$A_s(\vec{q}+\vec{G},z)=\int d^2r\, a^m_\nu(\vec{r}-\vec{R}^{\parallel}_m,z-R^z_m)e^{-i(\vec{q}+\vec{G})\cdot\vec{r}} \times a^{m'}_{\nu'}(\vec{r}-\vec{R}^{\parallel}_{m'}-\vec{R}_s,z-R^z_{m'}) . \tag{2.7}$$

The vector $\vec{q}$ is a two-dimensional (2D) vector in the irreducible part of the Brillouin zone and $\vec{G}$ is a 2D reciprocal-lattice vector. Moreover, $\vec{r}$ is a 2D vector parallel to the surface as well as $\vec{R}_s$ which is a translation vector. $\vec{R}^{\parallel}_m$ and R^z_m are the parallel and perpendicular components, respectively, of a 3D basis vector corresponding to the mth layer. The index ν gives the different orbitals. Finally, s is determined by the set of indices defined before: $s\equiv(\nu,\nu',m,m',R_s)$.[8,12]

The matrix $\tilde{S}_{ss'}$ is given in the time-dependent Hartree approximation by

$$\tilde{S}_{ss'}(\vec{q},\omega)=N_{ss'}(\vec{q},\omega) , \tag{2.8}$$

where $N_{ss'}$ was already defined in I. The corresponding diagram is shown in Fig. 3(a). In this approximation the polarizability $\tilde{\chi}$ contains only contributions from noninteracting electrons and holes. In the time-dependent

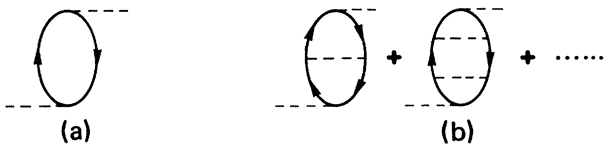

FIG. 3. (a) Hartree polarizability; (b) contribution from the electron-hole attraction in the time-dependent Hartree-Fock approximation.

screened Hartree-Fock approximation (TDSHF) we have

$$\tilde{S}_{ss'}(\vec{q},\omega)=[N^{-1}_{ss'}(\vec{q},\omega)+\tfrac{1}{2}V^{s}_{ss'}]^{-1}\ , \tag{2.9}$$

where V^s was also given in I. The diagrams corresponding to this approximation are shown in Fig. 3(b), where the interaction lines inside each bubble should be understood as a statically screened Coulomb attraction. The separability of the polarizability in Eq. (2.6) allows us to solve the integral equation (2.4), to obtain[17]

$$\chi(\vec{q}+\vec{G},\vec{q}+\vec{G}';z,z';\omega)=\sum_{ss'}A_s(\vec{q}+\vec{G},z)S_{ss'}(\vec{q},\omega)A^{\dagger}_{s'}(\vec{q}+\vec{G}',z')\ , \tag{2.10}$$

where

$$S_{ss'}(\vec{q},\omega)=(\tilde{S}^{-1}-V^{c})^{-1}_{ss'} \tag{2.11}$$

and

$$V^{c}_{ss'}=\sum_{\vec{G}}\int dz\,dz'A^{\dagger}_{s}(\vec{q}+\vec{G},z)v(\vec{q}+\vec{G},|z-z'|)\times A_{s'}(\vec{q}+\vec{G}',z')\ . \tag{2.12}$$

The expression (2.12) corresponds to the Coulomb interaction between the generalized charge-density waves A_s and $A_{s'}$.

We restrict ourselves to the TDSHF approximation, where $S_{ss'}$ is given by

$$S_{ss'}(\vec{q},\omega)=[N^{-1}(\vec{q},\omega)+V^{xc}(\vec{q})]^{-1}_{ss'} \tag{2.13}$$

with $V^{xc}(\vec{q})=-V^{c}(\vec{q})+\frac{1}{2}V^{s}(\vec{q})$.

B. Surface dynamical matrix

Having obtained the density-response function, we can now present a form of the surface dynamical matrix, which includes the electronic correlation effects discussed in I and in Sec. II A. We consider a thin slab with surfaces perpendicular to the z direction. The normal-mode solutions are of the form

$$u_{\alpha}(\kappa)=M^{-1/2}\xi_{\alpha}(\kappa,\vec{q})e^{i\vec{q}\cdot\vec{R}^{\parallel}_{\kappa}}e^{-i\omega t}\ , \tag{2.14}$$

where u_α is the α component of the displacement of the ion κ with mass M from its equilibrium position $\vec{R}^{0}_{\kappa}=(\vec{R}^{\parallel 0}_{\kappa},R^{z0}_{\kappa})$.

The electronic contribution to the second-order force constants is[16]

$$\phi^{E}_{\alpha\beta}\begin{bmatrix}\kappa\kappa'\\ ll'\end{bmatrix}=\int\int d^3r\,d^3r'\left[\frac{\partial W}{\partial r_\alpha}(\vec{r}-\vec{R}_l-\vec{R}^{0}_{\kappa})\chi(\vec{r},\vec{r}';\omega)\frac{\partial W}{\partial r'_\beta}(\vec{r}'-\vec{R}_{l'}-\vec{R}^{0}_{\kappa'})-\delta_{ll'}\delta_{\kappa\kappa'}\sum_{l''\kappa''}\frac{\partial W}{\partial r_\alpha}(\vec{r}-\vec{R}_l-\vec{R}^{0}_{\kappa})\chi(\vec{r},\vec{r}';\omega=0)\frac{\partial W}{\partial r'_\beta}(\vec{r}'-\vec{R}_{l''}-\vec{R}^{0}_{\kappa''})\right]\ , \tag{2.15}$$

where

$$W(\vec{r}-\vec{R}_l-\vec{R}^{0}_{\kappa})=-\frac{Z_\kappa e^2}{|\vec{r}-\vec{R}^{l}_{\kappa}|} \tag{2.16}$$

is the ionic potential experienced by an electron at position $\vec{r}$ due to an ion at position $\vec{R}^{l}_{\kappa}=\vec{R}_l+\vec{R}^{0}_{\kappa}$, $\vec{R}_l$ being a 2D translation vector. In the adiabatic approximation, the response function χ must be calculated in the static limit. The dynamical matrix is defined as the Fourier transform of the force constants. The electronic contribution has the following form:

$$D^{E}_{\alpha\beta}(\kappa\kappa',\vec{q})=\bar{D}^{E}_{\alpha\beta}(\kappa\kappa',\vec{q})-\bar{D}^{E}_{\alpha\beta}(\kappa\kappa',0)\ , \tag{2.17}$$

with

$$\bar{D}^{E}_{\alpha\beta}(\kappa\kappa',\vec{q})=(M_\kappa M_{\kappa'})^{-1/2}\sum_{ss'}F^{\alpha}_{s}(\kappa,\vec{q})S_{ss'}(\vec{q})F^{\beta\dagger}_{s}(\kappa',\vec{q})\ . \tag{2.18}$$

The factors $F^{\alpha}_{s}(\kappa,\vec{q})$ give the force in direction α on the ion κ at the site R^{0}_{κ} due to interaction with a charge-density wave A_s. The form of these force factors is the following:

$$F^{\alpha}_{s}(\kappa,\vec{q})=-i\sum_{\vec{G}}(\vec{q}+\vec{G})_\alpha e^{i\vec{G}\cdot\vec{R}^{\parallel 0}_{\kappa}}\times\int dz\,W(\vec{q}+\vec{G},|z-R^{z0}_{\kappa}|)\times A_s(\vec{q}+\vec{G},z) \tag{2.19a}$$

for $\alpha=x,y$ and

$$F^{z}_{s}(\kappa,\vec{q})=-\sum_{G}|\vec{q}+\vec{G}|e^{i\vec{G}\cdot\vec{R}^{\parallel 0}_{\kappa}}\times\int dz\,\mathrm{sgn}(z-R^{z0}_{\kappa})W(\vec{q}+\vec{G},|z-R^{z0}_{\kappa}|)\times A_s(\vec{q}+\vec{G},z)\ . \tag{2.19b}$$

Equation (2.18) shows how the phonon properties will be influenced by the electronic response. In particular, if an electronic instability appears, as was discussed in I, a great enhancement of the screening matrix $S(\vec{q})$ will result, which can drive a structural instability. In the next section we will show for the ideal Si(111) surface that charge-density fluctuations appear in connection with structural instabilities at the boundary of the Brillouin zone.

C. Effective charge for a metallic surface

As a complement to the microscopic formalism of surface lattice dynamics, we present here the expressions of surface effective charges. We deal in this section with a metallic system as in the case for the ideal Si(111) surface, the insulating case having been presented elsewhere.[11]

As in the insulating case, we must examine the long-wavelength behavior of the density-response function $\chi(\vec{q}+\vec{G},\vec{q}+\vec{G}';z,z';\omega=0)$. In the metallic case, the absence of a gap gives the following result:

$$\int dz'\chi(G,0;z,z';\omega=0)\neq 0 . \tag{2.20}$$

To proceed further, we define as in the insulating case a short-range part of the susceptibility,

$$\hat{\chi}(\vec{q}+\vec{G},\vec{q}+\vec{G}';z,z')=\tilde{\chi}(\vec{q}+\vec{G},\vec{q}+\vec{G}';z,z')+\sum_{G''\neq 0}\int\int dz_1dz_2\tilde{\chi}(\vec{q}+\vec{G},\vec{q}+\vec{G}'';z,z_1)$$
$$\times v(|\vec{q}+\vec{G}|;|z_1-z_2|)\hat{\chi}(\vec{q}+\vec{G}'',\vec{q}+\vec{G}';z_2,z') , \tag{2.21}$$

where

$$v(|\vec{q}+\vec{G}|;|z_1-z_2|)=2\pi e^2\frac{e^{-|\vec{q}+\vec{G}|\cdot|z_1-z_2|}}{|\vec{q}+\vec{G}|} \tag{2.22}$$

is the 2D Fourier-transformed Coulomb interaction and $\tilde{\chi}(\vec{q}+\vec{G},\vec{q}+\vec{G}';z,z')$ is the polarizability of the system. The susceptibility can then be obtained through the following integral equation:

$$\chi(\vec{q}+\vec{G},\vec{q}+\vec{G}';z,z')=\hat{\chi}(\vec{q}+\vec{G},\vec{q}+\vec{G}',z,z')+\int\int dz_1dz_2\hat{\chi}(\vec{q}+\vec{G},\vec{q};z,z_1)v(|\vec{q}|,|z_1-z_2|)\chi(\vec{q},\vec{q}+\vec{G}';z_2,z') . \tag{2.23}$$

If $q=0$, due to charge neutrality we can take $v(0,|z-z'|)=0$ (at least for a thin slab) and then

$$\chi(G,G';z,z')=\hat{\chi}(G,G';z,z') . \tag{2.24}$$

For $q\sim 0$ we can do the following expansion for the susceptibility:

$$\int\int dz\,dz'\chi(\vec{q},\vec{q};z,z')\simeq\frac{1}{\epsilon(\vec{q})}\int\int dz\,dz'\hat{\chi}(\vec{q},\vec{q};z,z') , \tag{2.25a}$$

$$\int\int dz\,\chi(\vec{q},\vec{q}+\vec{G}';z,z')\simeq\frac{1}{\epsilon(\vec{q})}\int dz\,\hat{\chi}(\vec{q},\vec{q}+\vec{G}';z,z') , \tag{2.25b}$$

$$\int\int dz'\chi(\vec{q}+\vec{G},\vec{q};z,z')\simeq\frac{1}{\epsilon(\vec{q})}\int dz'\hat{\chi}(\vec{q}+\vec{G},\vec{q};z,z') , \tag{2.25c}$$

$$\chi(\vec{q}+\vec{G},\vec{q}+\vec{G}';z,z')\simeq\hat{\chi}(\vec{q}+\vec{G},\vec{q}+\vec{G}';z,z')+\int dz_1\hat{\chi}(\vec{q}+\vec{G},\vec{q};z,z_1)\frac{v(q)}{\epsilon(q)}\int dz_2\hat{\chi}(\vec{q},\vec{q}+\vec{G}';z_2,z') , \tag{2.25d}$$

where

$$\epsilon(\vec{q})\equiv 1-v(q)\int\int dz\,dz'\hat{\chi}(\vec{q},\vec{q};z,z') \tag{2.26}$$

and

$$v(\vec{q})\equiv\frac{2\pi e^2}{|\vec{q}|} . \tag{2.27}$$

Now we insert the expansions (2.25a)–(2.25d) in the dynamical matrix and separate those terms with short-range contributions from those which could in principle have long-range behavior. Then we obtain the following form for the dynamical matrix, very similar to the bulk form:[18]

$$D_{\alpha\beta}(\kappa\kappa';\vec{q})=(M_\kappa M_{\kappa'})^{-1/2}\{e^{i\vec{q}\cdot\vec{R}_\kappa}q_\alpha[Z_\kappa Z_{\kappa'}v(q)-W(q,\kappa)W(q;\kappa')/v(q)]q_\beta e^{-i\vec{q}\cdot\vec{R}_{\kappa'}}$$
$$+e^{i\vec{q}\cdot\vec{R}_\kappa}Z_\alpha^\dagger(\vec{q};\kappa)[v(q)/\epsilon(q)]Z_\beta(q;\kappa')e^{-i\vec{q}\cdot\vec{R}_{\kappa'}}+\cdots\} \tag{2.28}$$

(where the ellipsis represents short-range terms), and where again

$$W(q,\kappa)\equiv\frac{2\pi e^2Z_\kappa}{|q|} , \tag{2.29}$$

and $\alpha,\beta=x,y$. The effective charge $Z_\alpha(\vec{q},\kappa)$ is defined following the result for bulk in Ref. 18:

$$Z_\alpha(\vec{q},\kappa)=-i\left[q_\alpha W(q,\kappa)/v(q)+\sum_{G\neq 0}(\vec{q}+\vec{G})_\alpha e^{-i\vec{G}\cdot\vec{R}_\kappa}\int\int dz\,dz'\hat{\chi}(\vec{q},\vec{q}+\vec{G};z,z')W(q+G;|z'-R_\kappa|)\right]. \quad (2.30)$$

For $\alpha=z$ we repeat the same procedure as before considering the element D_{zz} of the dynamical matrix and obtain

$$Z_z(q;\kappa)=|q|\frac{W(q,\kappa)}{v(q)}+\sum_{G\neq 0}|\vec{q}+\vec{G}|e^{-i\vec{G}\cdot\vec{R}_\kappa}\int\int dz\,dz'\hat{\chi}(\vec{q},\vec{q}+\vec{G};z,z') \times\mathrm{sgn}(z'-R_\kappa)W(\vec{q}+\vec{G};|z'-R_\kappa|). \quad (2.31)$$

The expressions (2.30) and (2.31) have the limit for $q\to 0$ (Ref. 18):

$$Z_\alpha(0,\kappa)=N^{-1}\int d^3r\int d^3r'\chi(\vec{r},\vec{r}')\sum_l -\frac{\partial W}{\partial r'_\alpha}(\vec{r}'-\vec{R}_{l\kappa};\kappa), \quad (2.32)$$

which is the change of the electronic charge density per unit displacement of the sublattice κ. We must point out here that a difficulty appears when dealing with $D_{\alpha z}$ or $D_{z\alpha}$ where $\alpha=x$ or y. In these cases we were not able to reduce the dynamical matrix to an expression such as (2.28). Further work is needed on this point.

III. RESULTS

In this section we study the lattice dynamics of the ideal Si(111) surface. The results were obtained by coupling the charge-density fluctuations, which were determined by the susceptibilities calculated in I, to the ionic system using the formation described in Sec. II.

We first study a 2D array of DB orbitals with the same configuration as in the topmost layer of the ideal Si(111) slab presented in I. There we showed that such a 2D system presents no electronic instabilities. The spectrum of the phonons corresponding to ionic motions parallel to the plane of the 2D system are shown in Fig. 4. The solid lines correspond to the bare-ion phonons, where the longitudinal branch presents a dispersion curve typical for a 2D plasmon ($\omega^2\propto q$), and the dashed line to the renormalized phonons. We observe that at the L point no renormalization of the phonon occurs, that is, the charge density wave (CDW) cannot couple to the lattice for $\vec{q}=\vec{G}/2$. By examining the force-form factor $F_\alpha(\vec{q})$ we can see that the symmetry of the DB orbitals on the (111) surface does not allow a coupling of the CDW to displacements parallel to the surface on a 2D model. To illustrate this behavior let us write $F_\alpha(\vec{q})$ in the following way:

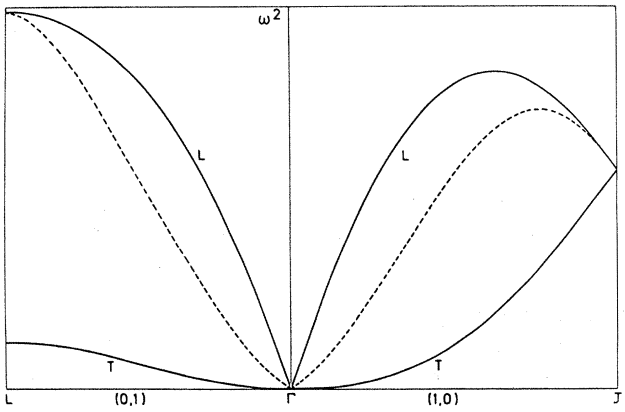

FIG. 4. Phonons of a 2D monolayer. The solid lines correspond to the longitudinal (L) and transverse (T) phonon branches for the system with "bare" ions. The dashed line results from the renormalization of the longitudinal branches by electronic screening.

$$F_\alpha(\vec{q})=\sum_{\vec{R}}e^{-i\vec{q}\cdot\vec{R}}F^\alpha_{0\vec{R}}, \quad (3.1)$$

where

$$F^\alpha_{0\vec{R}}=-\int d^3r\phi^*_\nu(\vec{r})\phi_\nu(\vec{r})\frac{\partial}{\partial r_\alpha}W(\vec{r}-\vec{R},z) \quad (3.2)$$

is the force experienced by an ion at lattice site $\vec{R}$ due to interaction with a charge density at site $\vec{R}=0$. If we take into account that the projection on the surface of the charge distribution of a DB orbital has a monopolar character, we obtain the following result for $\alpha=x,y$:

$$F_{00}=0, \qquad F_{0R}=-F_{0-R}. \quad (3.3)$$

Owing to this symmetry property of the DB orbitals on the (111) surface we obtain

$$F_\alpha(\vec{q}=\vec{G}/2)=\sum_{\vec{R}}e^{-i\vec{q}\cdot\vec{R}}F^\alpha_{0R}=0. \quad (3.4)$$

In Fig. 5(a) we show the coupling factor $F\times F^\dagger$ for displacements parallel to the surface in the direction Γ-L where we can observe that $F(\vec{q})=0$ for $q=G/2$. Displacements parallel to the surface can couple through the interaction between DB and "backbond" orbitals [Fig. 5(b)], but with much smaller amplitude.

The situation described above changes for a slab, where the 3D character allows for coupling of the DB orbitals with backbond orbitals and where restrictions imposed by symmetry properties of the 2D model are no longer present. The geometry and electronic properties of such a slab were already described in I and we will not repeat them here. In the following we briefly discuss details concerning the force-form factors F^α_s and then we present the results for the 3D case.

For the force-form factors F a pseudopotential of the form

$$W(\vec{r})=-\frac{e^2}{r}(1-\beta e^{-\alpha r}) \quad (3.5)$$

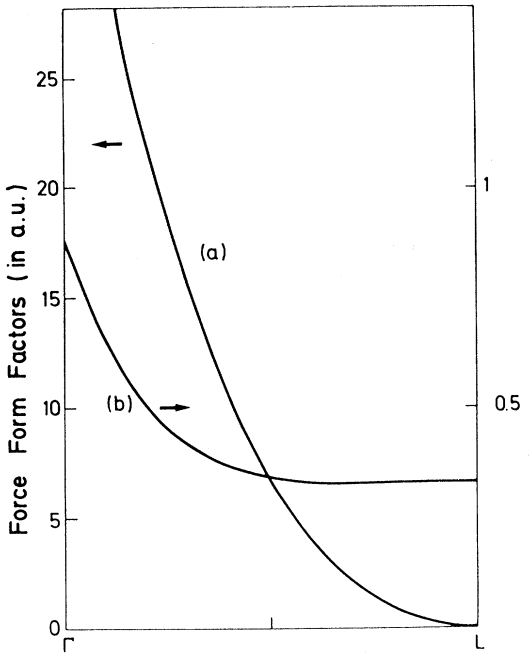

FIG. 5. Electron-phonon coupling form factor $F \times F^{\dagger}$: (a) for DB-DB interaction; (b) for DB backbond interactions, both for displacements parallel to the surface.

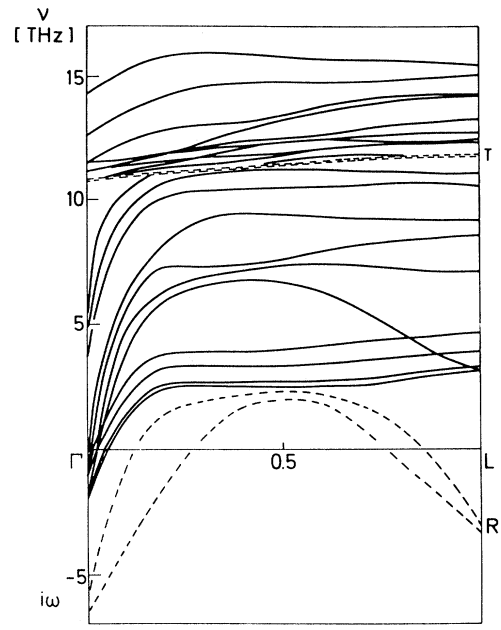

FIG. 6. Calculated phonon spectrum for an eight-layer slab. T: transverse optic surface modes. R: Rayleigh modes. The imaginary frequencies correspond to the unstable phonons.

was chosen. This pseudopotential corresponds to a frozen-core approximation where the only contributions to the polarizability come from the valence electrons. The constants α and β were adjusted in order to obtain the correct phonon bandwidth and their values ($\alpha=0.573$, $\beta=1.49$ in a.u.) are in the order of magnitude of the ones which can be obtained by fitting the ionic pseudopotential of Si given by Cohen and Heine.[19] The orthogonalization of the orbitals in the force-form factors was seen to be important for the stability of the phonons for long wavelengths. The antibonding orbitals were orthogonalized to the bonding orbitals using Löwdin's method,[20]

$$\tilde{\phi}^{a}_{\nu}(\vec{r})=\phi^{a}_{\nu}(\vec{r})-\sum_{\mu,\vec{R}}\langle\phi^{b}_{\mu}(\vec{r}-\vec{R})\,|\,\phi^{a}_{\nu}(\vec{r})\rangle\phi^{b}_{\mu}(\vec{r}-\vec{R})\,. \quad (3.6)$$

We neglect the contributions coming from orbitals sitting in different places and consider only terms first order in $t\equiv\langle\phi^{b}_{\mu}(\vec{r})\,|\,\phi^{a}_{\nu}(\vec{r})\rangle$. Owing to the fact that $\langle\phi_{\mu}(\vec{r})\,|\,\phi_{\mu}(\vec{r})\rangle\sim t$ and $\langle\phi_{\mu}(\vec{r})\,|\,\phi_{\nu}(\vec{r})\rangle=0$ we have, finally, the following correction:

$$\tilde{\phi}^{a}_{\nu}(\vec{r})\simeq\phi^{a}_{\nu}(\vec{r})-\langle\phi^{b}_{\mu}(\vec{r})\,|\,\phi^{a}_{\nu}(\vec{r})\rangle\phi^{b}_{\mu}(\vec{r})\,, \quad (3.7)$$

where ν and μ are determined by the index s in $F^{\alpha}_{s}(\vec{q},\kappa)$.

We present in Fig. 6 the phonon spectrum in the Γ-L direction calculated for an ideal Si(111) slab with eight layers. The dashed lines correspond to surface modes and the solid lines correspond to modes extended through the whole slab. In our work we designate as surface modes those modes which are localized in the first and second layers with amplitudes decaying approximately exponentially in directions perpendicular to the slab. The identification of resonant-mode results is very difficult because the slab is too thin. Moreover, the surface modes appear pairwise due to interactions between both surfaces of the slab.

Two kinds of surface modes are obtained. The low-energy modes, characterized with R in Fig. 6, appear below the bulklike modes and are elliptically polarized in the sagittal plane (in our case the y-z plane). Owing to these characteristics we identify them as Rayleigh modes.[21,22] The other modes are transverse modes, polarized parallel to the surface. Both modes were also obtained by Zimmermann[23] and Ludwig[24] with a phenomenological model for a semi-infinite Si crystal.

The Rayleigh modes present two different types of instabilities. In the region where $q \lesssim 1/l$, l being the thickness of the slab, we obtain phonon instabilities which are related to the fact that we are dealing with an unrelaxed surface (violation of infinitesimal rotational invariance[25]).

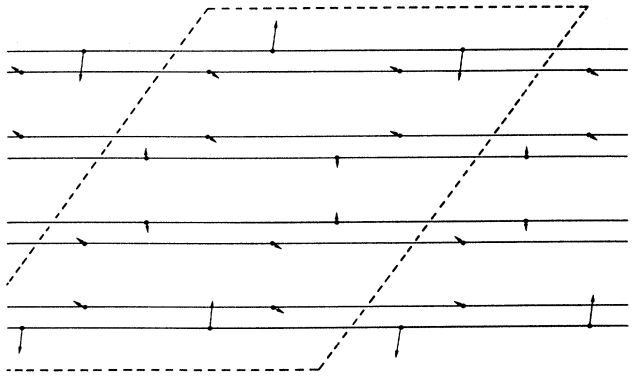

FIG. 7. Displacement pattern corresponding to the phonon instabilities of the L point. The dashed line shows the new unit cell for the 2×1 superstructure.

The Rayleigh-mode instabilities at the L point are a direct consequence of enhanced charge-density fluctuations which show in an incipient form in the susceptibility calculated in I. The soft phonon at the L point corresponds to a structural instability against a 2×1 superstructure. A study of the eigenvectors of this mode shows the displacement pattern of the atoms (Fig. 7).

IV. DISCUSSION

Based on a previous formulation of a many-body theoretical framework for the calculation of surface elementary excitations and response functions, we obtain expressions for the surface phonon self-energy and the surface dynamical effective charge. We apply this formalism to the study of the phonon spectrum of an eight-layer slab with ideal Si(111) surfaces. Two types of structural instabilities are found, both related to surface Rayleigh modes. One type of instability is found for small 2D wave vectors, which is due to the unrelaxed configuration of the slab. The other type of instability, given by the soft phonons at the zone boundary, is related to enhanced charge-density fluctuations which manifest in an incipient form in a previous study (I) we performed on electronic instabilities in the same system. This structural instability corresponds to a 2×1 superstructure. The displacement pattern of the atoms is given by the eigenvectors of the soft mode.

We should remark here that our results partly differ with total-energy calculations which show that buckling geometries raise the total energy with respect to the ideal configurations,[26] while others[27] apparently show a reduction of energy for some buckling configurations. We believe that the discrepancy between our results, which show an instability with a buckling geometry, and the local-density calculations is related to the difference in treatment of exchange and correlation near the surface, where nonlocality effects may become more important than in bulk. A more detailed investigation is needed in this direction.

ACKNOWLEDGMENT

This material is based upon research supported in part by the National Science Foundation under Grant No. PHY77-27084, supplemented in part by the National Aeronautics and Space Administration.

[1]See, for example, C. B. Duke, A. Paton, W. K. Ford, A. Kahn, and G. Scott, Phys. Rev. B **24**, 3310 (1981), and references therein.

[2]Recent references are H. Lüth, Physica **118B**, 810 (1983); H. Ibach and S. Lewald, J. Vac. Sci. Technol. **15**, 407 (1978); H. Raether, in *Solid State Excitations by Electrons,* Vol. 38 of *Springer Tracts in Modern Physics,* edited by G. Höhler and E. A. Niekisch (Springer, Berlin, 1965); J. M. Szeftel, S. Leckwald, H. Ibach, T. S. Rahman, J. E. Black, and D. L. Mills, Phys. Rev. Lett. **51**, 268 (1983).

[3]J. M. Horne and D. R. Miller, Phys. Rev. Lett. **41**, 511 (1978); G. Benedek, G. Brusdeyline, R. B. Doak, and J. P. Toennies, J. Phys. (Paris) Suppl. C **6-42**, 793 (1981).

[4]For a recent excellent review on surface waves, see A. A. Maradudin, in *Festkörperprobleme XXI—Advances in Solid State Physics,* edited by J. Treusch (Vieweg, Braunschweig, 1981), p. 15.

[5]W. Ludwig, in *Recent Developments in Lattice Theory,* Vol. 43 of *Springer Tracts in Modern Physics,* edited by G. Höhler and E. A. Niekisch (Springer, Berlin, 1967), p. 63; G. Benedek, Surf. Sci. **61**, 603 (1976); F. W. de Wette and G. P. Allredge, in *Method of Computational Physics,* edited by G. Gilat *et al.* (Academic, New York, 1976), Vol. 15, Chap. 5, p. 163.

[6]For a recent summary, see the various articles in Physica **118B**, pp. 761-862 (1983).

[7]T. E. Felter, R. A. Barker, and P. J. Estrup, Phys. Rev. Lett. **38**, 1138 (1977).

[8]A. Muramatsu and W. Hanke, preceding paper, Phys. Rev. B **30**, 1911 (1984).

[9]K. C. Pandey, Phys. Rev. Lett. **47**, 1913 (1981); **49**, 223 (1982); J. E. Northrup and M. L. Cohen, J. Vac. Sci. Technol. **21**, 333 (1982).

[10]He scattering experiments for Si surfaces are presently under study in Göttingen; J. P. Toennies (private communication).

[11]A. Muramatsu, Phys. Rev. B **24**, 4831 (1981).

[12]A. Muramatsu and W. Hanke, in *Ab-initio Calculations of Dynamical Properties of Solids,* edited by J. T. Devreese (Plenum, New York, 1982).

[13]P. Nozières, *Theory of Interacting Fermi Systems* (Benjamin, New York, 1964).

[14]W. Hanke and L. J. Sham, Phys. Rev. B **21**, 4656 (1980).

[15]V. Ambegaokar and W. Kohn, Phys. Rev. **117**, 423 (1960).

[16]L. J. Sham, Phys. Rev. **188**, 1431 (1969).

[17]C. H. Wu and W. Hanke, Solid State Commun. **23**, 829 (1977).

[18]L. J. Sham, Phys. Rev. B **6**, 3581 (1972).

[19]M. L. Cohen and V. Heine, Solid State Phys. **24**, 38 (1970).

[20]P. O. Löwdin, J. Chem. Phys. **18**, 365 (1950).

[21]S. Y. Tong and A. A. Maradudin, Phys. Rev. **181**, 1318 (1969).

[22]R. E. Allen, G. P. Alldredge, and F. W. de Wette, Phys. Rev. B **4**, 1661 (1971).

[23]R. Zimmermann, Appl. Phys. **3**, 235 (1974).

[24]W. Ludwig, Jpn. J. Appl. Phys. Suppl. 2, 879 (1974).

[25]W. Ludwig and B. Lengeler, Solid State Commun. **2**, 83 (1964); A. A. Maradudin, E. W. Montroll, G. H. Weiss, and I. P. Ipatova, *Theory of Lattice Dynamics in the Harmonic Approximation* (Academic, New York, 1971), p. 523.

[26]K. C. Pandey, Phys. Rev. Lett. **49**, 223 (1982).

[27]J. E. Northrup, J. Ihm, and M. L. Cohen, Phys. Rev. Lett. **47**, 1910 (1981).